JOURNAL OF BACTERIOLOGY, Oct. 2002, p. 5330–5338 Vol. 184, No. 19
0021-9193/02/$04.00+0 DOI: 10.1128/JB.184.19.5330–5338.2002

Interdependent Expression of the *ccoNOQP-rdxBHIS* Loci in *Rhodobacter sphaeroides* 2.4.1

Jung Hyeob Roh and Samuel Kaplan*

Department of Microbiology and Molecular Genetics, The University of Texas Health Science Center Medical School, Houston, Texas 77030

Received 19 April 2002/Accepted 30 June 2002

The *rdxBHIS* gene cluster of *Rhodobacter sphaeroides* 2.4.1, located downstream of the *ccoNOQP* operon encoding the cbb_3 cytochrome *c* oxidase, is required for the posttranscriptional modification of the cbb_3 cytochrome *c* oxidase. The cbb_3 cytochrome *c* oxidase is the main terminal oxidase under microaerobic conditions, as well as a component of the signal transduction pathway controlling photosynthesis gene expression. Because of the intimate functional and positional relationships of the *ccoNOQP* operon and the *rdxBHIS* gene cluster, we have examined the transcriptional activities of this DNA region in order to understand their expression and regulation. Northern blot analysis and reverse transcription-PCR, together with earlier complementation analysis, suggested that the *ccoNOQP-rdxBHIS* cluster is transcribed as *ccoNOQP-*, *ccoNOQP-rdxBH-*, *rdxBH-*, and *rdxIS*-specific transcripts. Multiple transcriptional start sites have been identified by primer extension analyses: five for *ccoN*, four for *rdxB*, and one for *rdxI*. Transcription from $P1_N$ of *ccoN* and $P1_B$ of *rdxB* is dependent on the presence of FnrL. LacZ fusion analysis support the above-described studies, especially the importance of FnrL. Expression of the *cco-rdx* cluster is closely related to photosynthesis gene expression, suggesting that transcript stoichiometry and presumably the stoichiometry of the gene products are critical factors in controlling photosynthesis gene expression.

In a series of published studies, we have demonstrated that the cbb_3 cytochrome *c* oxidase of *Rhodobacter sphaeroides* 2.4.1, in addition to its role as a terminal oxidase, is also a critical component of the signal transduction pathway which regulates the onset of photosynthesis gene expression (15–18, 20, 23). Mutations of the *ccoNOQP* operon lead to the induction of photosynthesis gene expression under aerobic conditions, and as a related but secondary effect, such mutations also lead to altered carotenoid accumulations (15–18, 20). Since the photosystem is normally repressed under aerobic conditions, we have proposed that the cbb_3 cytochrome *c* oxidase transduces an inhibitory signal as the result of electron transfer, which ultimately inhibits photosynthesis gene expression under high-oxygen conditions. We have also shown that the rate or volume of electron transfer through the cbb_3 cytochrome oxidase is inversely related to the expression levels of the photosynthesis genes (18). Ultimately, this signal transduction pathway terminates with the global regulators PrrBA, comprising a two-component activation system (2, 4, 5, 15).

The *rdxBHIS* (*ccoGHIS*/*fixGHIS*) cluster is located immediately downstream of the *ccoNOQP* operon (20, 22). RdxB is believed to be a membrane-localized ferredoxin-like protein containing a 2[4Fe-4S] motif (by analogy to RdxA [14]). RdxI is a new subfamily of the CPx-type ATPase that functions to maintain the activity and integrity of the cbb_3 cytochrome *c* oxidase, believed to be through maintenance of intracellular copper homeostasis (20). RdxH and RdxS possess no recognizable protein motifs or homologues (20). Inactivation of the *rdxBHIS* gene cluster also results in photosystem gene expression under aerobic conditions, suggesting that these proteins are involved, either directly or indirectly, in the same signal transduction pathway as the cbb_3 cytochrome *c* oxidase (16, 17, 20). RdxH, -I, and -S are involved in the pathway by or through which the maturation and/or stability of the cbb_3 cytochrome oxidase is maintained (20).

Previously, we reported that the RDXB1 mutant of *R. sphaeroides* 2.4.1, in which the *rdxB* gene was disrupted by insertion of a trimethoprim cassette, could be complemented only when both the *rdxBH* genes were present in *trans* (16). The *rdxI* and *rdxS* genes were not required for complementation of the RDXB1 mutant, suggesting the existence of an internal promoter for complete transcription of the *rdxBHIS* gene cluster.

Analysis of the *fixGHIS* (*rdxBHIS*) cluster of *Sinorhizobium meliloti* suggested that *fixGHIS* constitutes a single transcription unit (7). The genes of the *ccoGHIS* (*rdxBHIS*) cluster of *Rhodobacter capsulatus* were reported to be expressed independently from one another (9). However, the growth of a *ccoGHIS* deletion mutation of *R. capsulatus* was not fully complemented by the *ccoGHIS* cluster but only by both the *ccoNOQP* and *ccoGHIS* gene clusters (9).

Because of the importance of the *rdxBHIS* gene cluster to photosynthesis gene expression and carotenoid biosynthesis, its relation to the expression of the cbb_3 cytochrome *c* oxidase, and the apparent disparity of homologous gene expression in other closely related bacteria, we have undertaken a thorough analysis of the transcriptional control of this region in *R. sphaeroides* 2.4.1.

* Corresponding author. Mailing address: Department of Microbiology and Molecular Genetics, The University of Texas Health Science Center Medical School, 6431 Fannin St., Houston, TX 77030. Phone: (713) 500-5502. Fax: (713) 500-5499. E-mail: samuel.kaplan@uth.tmc.edu.

MATERIALS AND METHODS

Bacterial strains, plasmids, and growth conditions. The *R. sphaeroides* and *Escherichia coli* strains and plasmids used in this study are described in Table 1. *E. coli* strains were grown at 37°C on Luria-Bertani medium supplemented, when

TABLE 1. Bacterial strains and plasmids used in this study

Strain or plasmid	Relevant characteristic(s)	Reference or source
E. coli		
DH5α*phe*	DH5α *phe*::Tn*10d*Cm	5
S17-1	C600::RP4-2(Tc::Mu)(Km::Tn*7*)*thi pro hsdR recA* Tra^+	21
R. sphaeroides		
2.4.1	Wild type	W. Sistrom
CCOP1	2.4.1 derivative, *ccoP*::ΩTp^r	16
JZ722	2.4.1 derivative, end of *ccoN*::Tn*5*TpMCS	23
JZ1678	2.4.1 derivative, Δ*fnrL*::ΩKm^r	22
Plasmids		
pRK415	Tc^r; Mob^+ *lacZ*α IncP	8
pGEM-T	Ap^r; TA cloning vector	Promega
pCF1010	Tc^r; Sm^r; Sp^r; IncQ/IncP4, promoter cloning vector	12
pJR194	pGEM-T::979 bp upstream of *rdxB*	This study
− 380	pGEM-T::380 bp upstream of *rdxB*	This study
− 112	pGEM-T::112 bp upstream of *rdxB*	This study
pUI1970	pRK415::*fnrL*	24
pUI2803	pRK415::4.7-kb *Bam*HI + *Eco*RI containing *ccoNOQP*	16
pUI2805	pRK415::4.2-kb *Pst*I + *Bam*HI containing *rdxBHI′*	16
pJR103	pRK415::4.9-kb *Pst*I fragment containing *rdxBHIS*	This study
pJR235	pRK415::8.3-kb *Bam*HI + *Pst*I containing *ccoNOQP-rdxBHIS*	This study
pJR471	pRK415::2.9-kb *Eco*O109I + *Pst*I containing *rdxH′IS*	This study
pJR473	pRK415::8.1-kb *Bam*HI fragment containing *ccoNOQP-rdxBHI′*	This study
pJR316	pCF1010::380 bp upstream of *rdxB*	This study
pJR319	pCF1010::112 bp upstream of *rdxB*	This study
pJR320	pCF1010::753 bp upstream of *rdxH*	This study
pJR321	pCF1010::442 bp upstream of *rdxI*	This study
pJR322	pCF1010::805 bp upstream of *rdxS*	This study

required, with tetracycline at 10 μg/ml and ampicillin, streptomycin, and spectinomycin at 50 μg/ml each. *R. sphaeroides* strains were grown at 30°C on Sistrom's minimal medium A containing succinate as a carbon source. Final concentrations of antibiotics were 1 μg/ml for tetracycline and 50 μg/ml for kanamycin, trimethoprim, streptomycin, and spectinomycin. Aerobic cultures were sparged with 30% O_2–69% N_2–1% CO_2. Photosynthetic cultures were grown at a light intensity of 30 W/m^2 and sparged with 95% N_2–5% CO_2. Growth of *R. sphaeroides* was monitored by measuring the optical density at 600 nm (OD_{600}) with a Shimadzu UV-1601PC spectrophotometer. Plasmids pRK415 and pCF1010 were used for gene expression and as a promoter-cloning vector for *R. sphaeroides,* respectively.

DNA manipulation and analysis. Standard protocols or manufacturer's instructions were followed to isolate plasmid DNA as well as for restriction enzyme treatment. DNA fragments containing the *rdxBH*, *rdxIS*, *rdxBHIS*, *ccoNOQP*, and *ccoNOQP-rdxBH* genes were subcloned under *tet* promoter control of pRK415 (Table 1). Plasmids were mobilized by biparental or triparental mating from *E. coli* strains into *R. sphaeroides.* Promoter regions for *rdxBHIS*::*lacZ* construction were amplified using PCR and subcloned into the pGEM-T plasmid (Promega). The plasmid pJR194 for *rdxB* was prepared with primer 52 (5′-CCG GAT CCC TGG GCC ATC GGC TAT TCG A-3′, extending from position −979 to −960 of *rdxB*) with a *Bam*HI site and a reverse primer (5′-CCT CTA GAG ATC CAC CAC TTC AGC CTG C-3′, extending from position +102 to +83 of *rdxB*). This DNA construct was subjected to nested deletion analysis. The 5′-deletion constructs −380 and −112 were created by exonuclease III digestion of pJR194 linearized with *Bam*HI and *Sac*I by using the Erase-A-Base system (Promega) according to the manufacturer's instructions. For the *rdxH*::*lacZ* construction, primer 82 (5′-CCA TGC ATG ATG GAC GAG GAG ACG ATC A-3′, extending from position −753 to −732 of *rdxH*) and primer 81 (5′-CCT CTA GAG CAG GTT CAC CGC GAT GAT-3′, extending from position +76 to +58 of *rdxH*) were used. The *rdxI*::*lacZ* fusion was prepared with primer 83 (5′-CCC TGC AGC AAG GTT CTG GCG ATC ACC-3′, extending from position −442 to −423 of *rdxI*) and primer 84 (5′-CCA TGC ATG TTC GGC GGA AGG TGC GGC-3′, extending from position +94 to +76 of *rdxI*). The *rdxS*::*lacZ* fusion was constructed with primer 85 (5′-CCC TGC AGC ACC AAT CTC GCG ACG CTT-3′, extending from position −805 to −787 of *rdxS*) and primer 86 (CCA TGC ATA GGA AGA GCG AGA TCG GGA-3′, extending from position +41 to +23 of *rdxS*). The PCR-amplified DNA fragments were confirmed by sequencing and subsequently subcloned into pCF1010.

Enzyme assay. Assays of β-galactosidase were performed on crude cell extracts of *R. sphaeroides* as previously described (20) at least twice, with standard deviations not exceeding 20%. Protein concentrations were determined with the Pierce (Rockford, Ill.) bicinchoninic acid protein assay reagent with bovine serum albumin as a standard.

RNA manipulation. Total RNA from *R. sphaeroides* was isolated by the acidic hot-phenol method. *R. sphaeroides* grown with sparging as described above was harvested at 6,000 × *g* for 4 min after the addition of rifampin (200 μg/ml). Pellets were resuspended in 3 ml of lysis solution (0.15 M sucrose, 10 mM sodium acetate [pH 4.7], 1% sodium dodecyl sulfate), which was preheated at 65°C. The lysate was transferred immediately to a 15-ml disposable polypropylene tube containing 3 ml of acidic phenol (pH 4.3) preheated to 65°C. The lysis mixture was maintained at 65°C for 10 min and carefully inverted several times. After centrifugation at 6,000 × *g* for 15 min, the lysis mixture was subjected to repeated acidic phenol extraction as described above. After centrifugation, the supernatant was transferred to a new tube containing phenol-chloroform-isoamyl alcohol (125:24:1, pH 4.3), mixed, and centrifuged as described above. The upper phase was extracted with chloroform-isoamyl alcohol (24:1). RNA was ethanol precipitated after centrifugation. The RNA pellets were washed with 70% ethanol, slightly dried, and resuspended in diethylpyrocarbonate-treated H_2O. To remove chromosomal DNA contamination, 40 U of RQ1 RNase-free DNase (Promega) was added to the RNA solution and incubated at 37°C for 1 h. RNA was precipitated by adding the same volume of 4 M LiCl after acidic phenol extraction as described above. Purified total RNA was separated by formaldehyde-containing agarose gel electrophoresis and transferred to a positively charged nylon membrane, BrightStar-Plus (Ambion). Strand-specific antisense RNA probes using [γ-^{32}P]CTP were prepared according to the manufacturer's instructions with an RNA transcription kit (Promega). Labeled probes (10^6 cpm/ml) were added to QuickHyb hybridization solution (Stratagene). Membrane hybridization and washing were performed according to the manufacturer's instructions. A portion of the 23S rRNA (0.4-kb *Hin*dIII-*Pst*I fragment) that is processed to 14S rRNA was used as a control for RNA normalization and standardization.

RT-PCR. Coupled reverse transcription-PCR (RT-PCR) was performed to investigate transcription of the *ccoNOQP-rdxBHIS* gene cluster. To remove chromosomal DNA contamination, 100 μg of total purified RNA was further incubated with 40 U of RQ1 RNase-free DNase (Promega) at 37°C for 40 min. The reaction mixture was extracted with acidic phenol (pH 4.3), phenol-chloroform-isoamyl alcohol, and chloroform-isoamyl alcohol as described above for total RNA isolation. RNA was ethanol precipitated after the supernatant was transferred to a new tube. The RNA pellets were washed with 70% ethanol and resuspended in diethylpyrocarbonate-treated water. First-strand cDNA was synthesized from 10 μg of total RNA prepared as described above by using the SuperScript II RNase H$^-$ reverse transcriptase (Invitrogen) at 45°C for 1 h with oligonucleotide a (5′-AGG CTG CTG GTT TGG GTA TC-3′, extending from position +32 to +12 of the *rdxB* gene). One-fourth of the total cDNA was then PCR amplified with LA *Taq* polymerase (Takara) by using primers b (5′-CCG ATC CGC GCC GTG AAT GAT-3′, extending from position −112 to −92 of *rdxB*), c (5′-TCA CCC ACG GCA TCC GCA-3′, extending from position +470 to +488 of *ccoP*), d (5′-TAC AGC CTG CTG CGT GGC-3′, extending from position +10 to +27 of *ccoQ*), and e (5′-CCG TTC CCG CTG AGT GAA-3′, extending from position +1592 to +1609 of *ccoN*).

For each RT-PCR experiment, three control experiments were performed: one without template to detect contamination, one with the RNA template but without the reverse transcriptase to ensure that there was no trace DNA, and one with pRK415 containing the *ccoNOQP-rdxBHIS* genes (pJR235) as a positive control for PCR amplification.

Primer extension. Total RNA was purified as described above and spectrophotometrically quantified. Primers for reverse transcription were end labeled with [γ-^{32}P]ATP and T4 polynucleotide kinase (Invitrogen). The primer labeling reaction included 20 pmol of the primer in a mixture of 39 μl of H_2O, 5 μl of [γ-^{32}P]ATP (3,000 Ci/mmol), 5 μl of 10× buffer, and 1 μl of T4 polynucleotide kinase. The reaction mixture was incubated for 1 h at 37°C. The unincorporated ATP was separated from the primer by using a Micro Bio-Spin P-30 column (Bio-Rad). Labeled primer containing 10^6 cpm and 10 μg of total RNA was mixed in 24 μl of H_2O, incubated at 70°C for 10 min, and chilled on ice. Reverse transcription was performed by mixing 8 μl of 5× reaction buffer, 4 μl of 0.1 M dithiothreitol, 2 μl of 1-mg/ml actinomycin D, 1 μl of 10 mM deoxynucleoside triphosphates, 1 μl of RNase inhibitor (SUPERase-In; Ambion), and 1 μl of SuperScript II RNase H$^-$ reverse transcriptase (Invitrogen). After 1 h of incubation at 45°C for extension, the enzyme was inactivated by heating at 70°C for 15 min and ethanol precipitated, and products were separated on an 8% sequencing gel next to a DNA sequencing reaction performed with the same primer. The specific signals revealed by Northern blotting as well as primer extension analyses were scanned and quantitated using NIH Image 1.62 software. Quantification was performed by subtracting the background level for each lane from the specific band.

RESULTS

The *ccoNOQP-rdxBHIS* cluster constitutes a variable transcriptional unit. (i) The *rdxBHIS* cluster. Although the *rdxBHIS* genes from *R. sphaeroides* 2.4.1 are tightly clustered and possess the same transcriptional polarity, we suggested previously that an internal promoter might exist within the *rdxBHIS* gene cluster (16). Complementation experiments showed that an RDXB1 mutant (*rdxB*::ΩTp^r) could be complemented with an *rdxBH*-containing DNA fragment but not with the *rdxB* gene alone and thus did not require the *rdxIS* genes (16). To ascertain the transcriptional activity of the *rdxBHIS* gene cluster in *R. sphaeroides* 2.4.1, we performed Northern blot analysis using total RNA derived from cells grown under phototrophic conditions. As shown in Fig. 1, the *rdxBHIS* cluster in the wild type produced several different transcription products which hybridized with different probes from the region, suggesting that the *rdxBHIS* gene cluster does not form a simple transcriptional unit. Although the transcripts appeared to be relatively unstable, as noted by the extent of smearing, the largest transcript (~5.7 kb) as well as a broad zone of degraded mRNA species from the wild type was observed with both the *rdxB* and *rdxH* riboprobes. The band at 5.7 kb was not observed

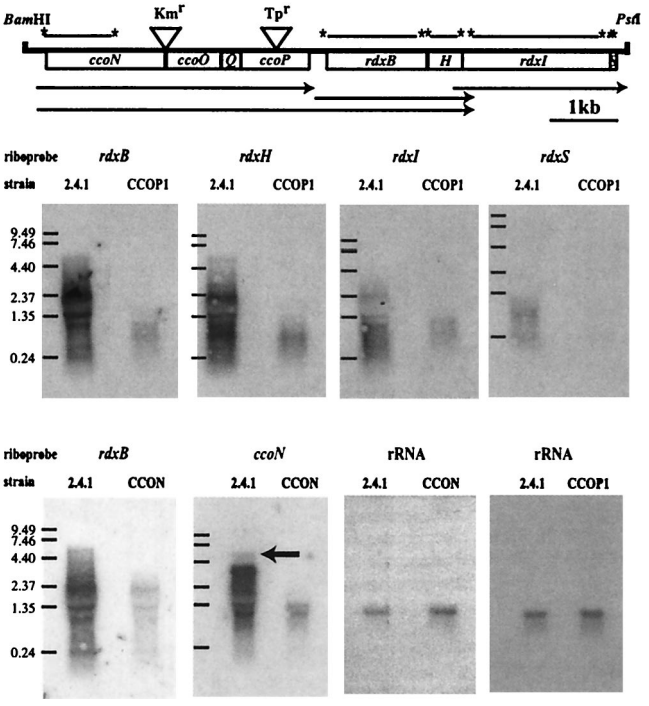

FIG. 1. Northern blot analysis of the *ccoNOQP-rdxBHIS* gene cluster. Total RNA was isolated from *R. sphaeroides* 2.4.1 and the *ccoN*::Km (CCON) and *ccoP*::Tp (CCOP1) mutants grown under phototrophic conditions. Insertion of the Km^r and Tp^r cassettes within the *ccoN* and *ccoP* genes, respectively, is indicated. Labeled lines with asterisks above the open bar designate the 5′ and 3′ ends of the riboprobes used. The arrows under the open bar indicate the deduced transcripts. The 3,434-bp *ccoNOQP* operon (1,608, 725, 204, and 873 bp, respectively) and the 4,268-bp *rdxBHIS* gene cluster (1,434, 459, 2,214, and 159 bp, respectively) are separated by 235 bp. Approximately 10 μg of total RNA was loaded onto each lane. The ^{32}P-labeled riboprobes corresponding to the *rdxB*, *rdxH*, *rdxI*, *rdxS*, *ccoN*, and 23S rRNA genes were used for hybridization as described in Materials and Methods. Molecular size ladders are shown to the left. The arrow in the *ccoN* hybridization panel indicates the transcript corresponding to the position of the longest transcript which was observed with the *rdxB* and *rdxH* riboprobes.

with the *rdxI* or *rdxS* riboprobe. Extending the exposure with the *rdxS* probe revealed the same transcript pattern as that of the *rdxI* probe (data not shown). The *rdxB*, *rdxH*, *rdxI*, and *rdxS* probes hybridized to longer transcripts (approximately 5.7 kb for *rdxB* and *rdxH* and 2.5 kb for *rdxI* and *rdxS*) than their expected gene sizes (20), namely, 1.434, 458, 2,213, and 158 bp, respectively. Because the size of the *rdxBHIS* cluster is approximately 4.3 kb and the longest transcript which showed a signal with either the *rdxB* or *rdxH* probe was not detected with the *rdxI* and *rdxS* probes, we conclude that *rdxBH* and *rdxIS* are transcribed differentially. These results suggested that the longer transcripts containing *rdxB* and *rdxH* contain all or part of the *ccoNOQP* operon, which is located immediately upstream of the *rdxBHIS* cluster and which is in the same transcriptional orientation. If there is an *rdxBHIS* transcript, it is of low abundance and very unstable.

(ii) *ccoNOQP* and *rdxBHIS*. To determine if the *ccoNOQP* and the *rdxBH* genes form a cotranscript, Northern blot analysis using RNA extracted from the CCOP1 mutant (16), in

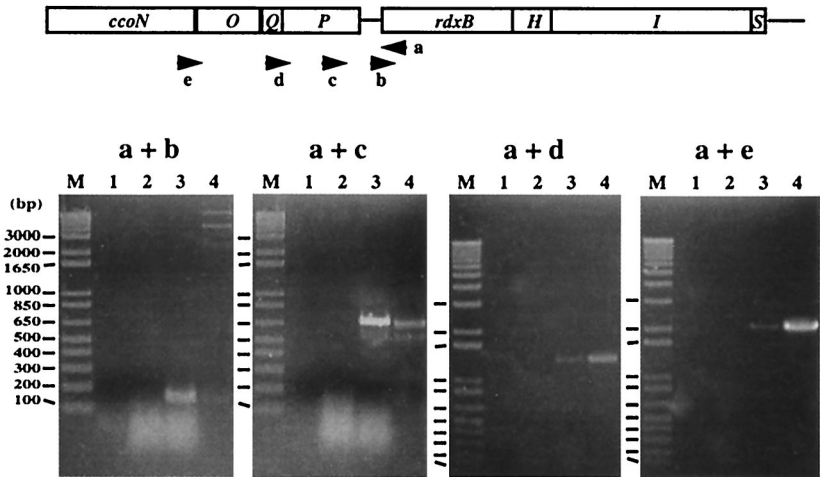

FIG. 2. RT-PCR of *R. sphaeroides* 2.4.1 total RNA. The locations of the oligonucleotides used for RT-PCR are shown by the arrows. The PCR products amplified by using the primers a, b, c, d, and e were subjected to electrophoresis on a 1% agarose gel (PCR product with primers a plus d and a plus e) or a 2% agarose gel (PCR products with primers a plus b and a plus c). The positions and sizes of the 1-kb plus DNA ladder from Invitrogen are indicated to the left (lanes M). The RT-PCR lacking a template failed to detect any contamination (lane 1), and total RNA without reverse transcriptase also failed to detect DNA contamination in the template (lanes 2), with the cDNA sample (lanes 3), and with positive control DNA, i.e., pJR235 containing the *ccoNOQP-rdxBHIS* genes in pRK415 (lanes 4).

which the *ccoP* gene is disrupted by an ΩTp^r cassette (Fig. 1), was performed. As demonstrated in Fig. 1, insertion of an ΩTp^r cassette into the *ccoP* gene resulted in a significantly reduced size and amount of the *rdxBHIS* transcript(s), thereby suggesting that transcription of the *rdxBHIS* genes is dependent primarily upon transcription that is initiated upstream of the ΩTp^r cassette, i.e., within *cco*.

Because the longest (~5.7-kb) transcript containing both the *rdxB* and *rdxH* genes has a size similar to the expected size of a transcript extending from the start of *ccoN* to the end of the *rdxH* protein-coding sequence (5,562 bp), we suggest that the *ccoNOQP* and *rdxBH* genes are for the most part transcribed as a single transcription unit. To confirm this hypothetical organization, transcriptional analysis was performed with total RNA isolated from the wild type and strain JZ722 (CCON), which contains a Tn*5*TpMCS cassette inserted between the *ccoN* and *ccoO* genes (23). We assumed that if cotranscription of *ccoNOQP-rdxBH* exists, the transcript size of the *rdxB* gene would be changed in mutant CCON, as was the case for the CCOP1 mutant, compared to the size of the transcript obtained by using both *rdxB* and *ccoN* as probes of the wild-type 2.4.1 RNA.

As shown in Fig. 1, when *rdxB* was used as a hybridization probe, significantly reduced transcript levels were observed in CCON. When the *ccoN* gene was used as a hybridization probe, we detected a 3.6-kb *ccoNOQP* transcript in the wild-type strain in addition to the same transcripts that were detected when *rdxB* was used as a probe. The 5.7-kb transcript detected with the *ccoN* and *rdxB* probes is best explained by cotranscription of *ccoNOQP-rdxBH* under photosynthetic conditions, again suggesting that expression of the *rdx* cluster is dependent primarily upon the upstream *cco* operon. The rRNA transcript was readily detected in relatively similar amounts in both strains.

(iii) RT-PCR. To further confirm the existence of a single transcript containing *ccoNOQP-rdxBH*, RT-PCR was performed with a set of oligonucleotides hybridizing to the 5′-untranslated region of *rdxB* (b) in addition to regions of the *cco* operon (c, d, and e) and oligonucleotide a, hybridizing to the *rdxB* gene (Fig. 2). PCR products of the expected sizes, i.e., 144 bp for primers a plus b, 670 bp for primers a plus c, 1,330 bp for primers a plus d, and 2,110 bp for primers a plus e, were obtained (Fig. 2). No PCR products were detected in any of the control reactions that were designed to detect DNA contamination. Although RT-PCR with the *rdxH*-specific primer was not performed, the Northern data showed that the *rdxH* gene was included in the longer (~5.7-kb) transcript containing the *ccoNOQP* operon.

Cotranscription of the *ccoNOQP-rdxBH* genes was also supported from Northern blot analysis using total RNA of an RDXI mutant in which approximately 1.5 kb of the *rdxI* gene was deleted in frame (20). The 5.7-kb band which was observed with the *rdxB*, *rdxH*, and *ccoN* probes was still observed in the RDXI mutant (data not shown).

Because the RT-PCR, Northern blot analysis, and earlier complementation experiments all support cotranscription of *ccoNOQP-rdxBH,* we went on to characterize the promoter regions of these gene clusters in order to better understand their expression and regulation.

Promoter structure of the *ccoNOQP* operon, *rdxB*, and *rdxI*. **(i) *ccoNOQP*.** To begin to understand the promoter structure of the *ccoNOQP* operon, we performed primer extension analysis using total RNA isolated from wild-type cells grown under aerobic and photosynthetic conditions. We also used total RNA prepared from strains that contained the *ccoNOQP* (pUI2803) and *ccoNOQP-rdxBH* (pJR473) genes in the multicopy plasmid pRK415. The oligonucleotides used for these experiments are indicated in Fig. 3C. Transcriptional start points were determined when different primers were used to detect the same transcripts in the primer extension experiments and when transcript abundance was correlated to the presence of extra copies of the corresponding genes. Specific

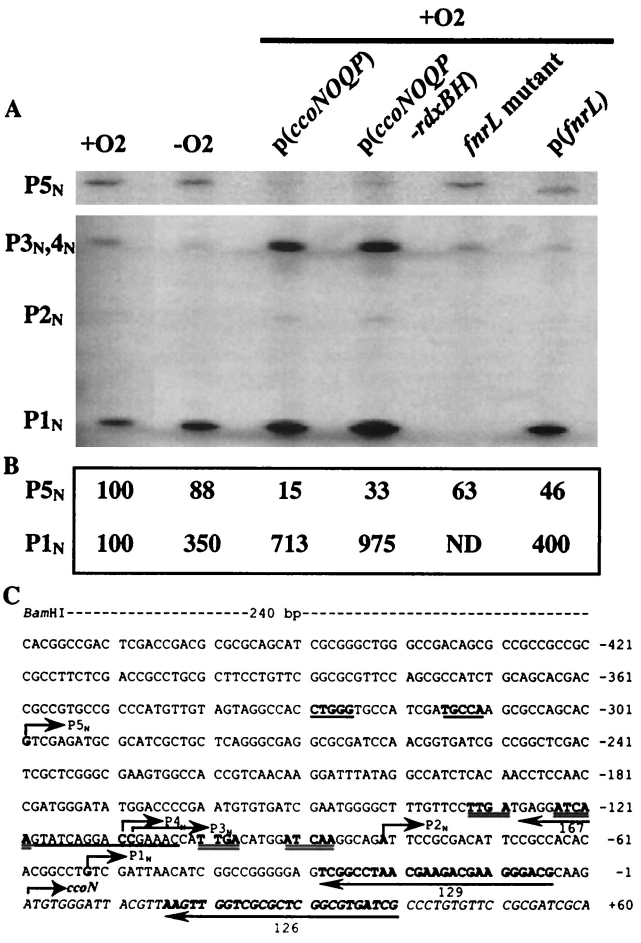

FIG. 3. Primer extension experiments and nucleotide sequence upstream of the *ccoN* gene. (A) Total RNAs isolated from the wild type grown under aerobic conditions ($+O_2$) and under photosynthetic conditions ($-O_2$), the wild type containing *ccoNOQP* in pRK415 [p(*ccoNOQP*)], the wild type containing *ccoNOQP-rdxBH* in pRK415 [p(*ccoNOQP-rdxBH*)], the *fnrL* mutant, and the wild type containing the *fnrL* gene in pRK415 [p(*fnrL*)] were used for primer extension experiments with primer 126. The 5′ ends ($P1_N$ to $P5_N$) are indicated on the left. Sizes of the primer extension products were determined by comparison to the sequencing ladder obtained from the same primer. $P3_N$, $P4_N$, and $P5_N$ were confirmed by extended gel electrophoresis (data not shown). (B) Quantification of signal levels of $P1_N$ and $P5_N$. Since the level of $P2_N$ was very low and the bands for $P3_N$ and $P4_N$ are indistinguishable, we did not quantitate these signals. The levels of $P1_N$ and $P5_N$ of wild-type cells grown aerobically were considered to be 100%, and other values are given relative to that value. ND, not detectable. (C) Nucleotide numbering is relative to the putative translational start site (designated +1) of the *ccoN* gene, which is shown in italics. The binding sites of the primers used in the primer extension experiments are underlined with arrows, and the number under the arrow is the primer number used for the experiment. The 5′ ends and directions of transcription are marked by arrows above the determined 5′ ends and are indicated as $P1_N$, $P2_N$, $P3_N$, $P4_N$, and $P5_N$. The *Bam*HI site was used in order to subclone the *ccoNOQP* operon into pRK415. Two putative FnrL binding sites are double underlined. A putative σ^{54} motif is indicated by an underline. The nucleotides mentioned above are in boldface, except the sequence for primer 167.

signals ($P1_N$ to $P5_N$) for the *ccoN* gene were obtained with oligonucleotides 126 and 129. The results of the primer extension experiments demonstrated the presence of a major signal located at −53 bp ($P1_N$) upstream of the *ccoN* translational start codon (Fig. 3A). An additional four 5′ ends, which showed weaker signals, were observed at −82 bp ($P2_N$), −109 bp ($P3_N$), −110 bp ($P4_N$), and −300 bp ($P5_N$). The 5′ ends were designated $P1_N$, $P2_N$, $P3_N$, $P4_N$, and $P5_N$, in order, from the *ccoN* translational start codon (Fig. 3A and C). Primer 167 confirmed the presence of the $P5_N$ transcript (data not shown). As shown in Fig. 3A and B, an approximately 3.5-fold-increased level of $P1_N$ was obtained when total RNA was derived from cells grown under photosynthetic conditions (lane 2) rather than under aerobic conditions (lane 1). The bands for $P2_N$, $P3_N$, and $P4_N$ were faint under both conditions. $P5_N$ was expressed at significantly greater levels than $P2_N$, $P3_N$, and $P4_N$, but much less than $P1_N$, under both growth conditions. Introduction of extra copies of the *ccoNOQP* operon under aerobic conditions caused significantly increased levels of $P1_N$, $P3_N$, and $P4_N$, but $P5_N$ decreased (Fig. 3A and B, lanes 3 and 4), perhaps suggesting an autoregulatory effect upon the $P5_N$ 5′ end. Thus, extra copies of *ccoNOQP* and *ccoNOQP-rdxBH* gave the same (but amplified) 5′ ends (except $P5_N$) as when they were present in single copy.

The *ccoNOQP* promoter region was analyzed to predict the possible DNA elements involved in its regulation. Previously, two putative FnrL binding motifs were described for the sequence upstream of the *ccoN* gene (13) (Fig. 3C). The FnrL binding motifs are centered at positions −73.5 and −41.5 from $P1_N$. Since β-galactosidase activity for a *ccoN*::*lacZ* fusion was significantly reduced in the *fnrL* mutant, it was suggested that FnrL is a major regulator of *ccoNOQP* expression (13). When total RNA was prepared from the *fnrL* mutant (lane 5) as well as from an *fnrL*-overexpressing strain (lane 6), we observed that transcription from $P1_N$ was absolutely dependent on the presence of FnrL. This is consistent with a role for FnrL as an activator of *ccoNOQP* expression and further supports the role of the $P1_N$ start site.

(ii) *rdxB* and *rdxI*. As demonstrated from the Northern blot analysis using CCOP1 and CCON in Fig. 1, transcription from the *cco* promoter constitutes the major regulatory region leading to the expression of *rdxBH*. In addition, the regions responsible for expression of *rdxB* and *rdxI* were also mapped by primer extension analysis because transcription of *rdxBH* and *rdxIS* was suggested earlier (Fig. 4A and B). Total RNA was prepared from strains containing plasmids pJR103, pUI2805, and pJR471, which contain the *rdxBHIS*, *rdxBH*, and *rdxIS* genes in pRK415, respectively, in addition to the wild-type strain. Four 5′ ends for *rdxB* were identified, at −23 bp ($P1_B$), −111 bp ($P2_B$), −116 bp ($P3_B$), and −134 bp ($P4_B$) upstream of the translational initiation site of the *rdxB* gene (Fig. 4C). Using extra copies of the *rdxBH* genes (Fig. 4A, lanes 2 and 6), we detected increased levels of these signals, supporting the results obtained for the wild type (Fig. 4A, lanes 1 and 4). Because the minor bands showed no alternations under any conditions, these were not considered significant. Total RNA isolated from the *fnrL* mutant (lanes 3 and 5) was also used to investigate the effect of FnrL on these 5′ ends, since a putative FnrL binding motif was found in the *rdxB* upstream region. The transcription level from $P1_B$ in the *fnrL* mutant was significantly reduced, suggesting positive regulation by FnrL, while the level was significantly increased with extra copies of *rdxBH* (lane 6).

Using the same approach with *rdxBHIS* and *rdxIS*, we de-

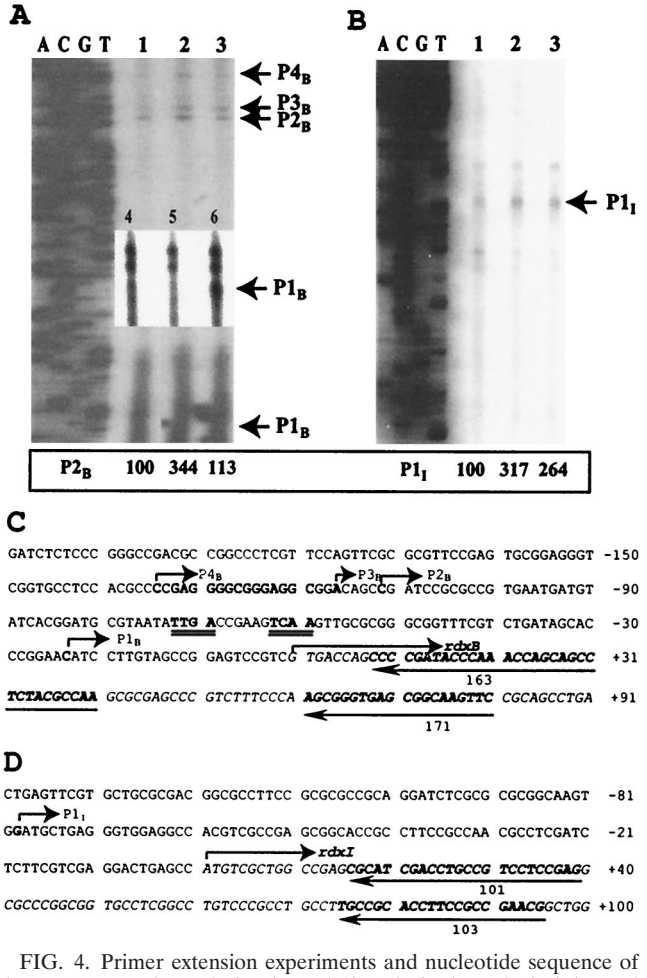

FIG. 4. Primer extension experiments and nucleotide sequence of the upstream regions of *rdxB* (A and C) and *rdxI* (B and D). (A) Total RNAs isolated from the wild type (lanes 1 and 4), the wild type containing the *rdxBH* genes in pRK415 (lanes 2 and 6), and the *fnrL* mutant (lanes 3 and 5) were used for primer extension experiments. The strains were grown under aerobic conditions. The levels of $P2_B$ and $P1_I$ of the wild type were considered to be 100%, and other levels are compared to these values. The $P1_B$ transcript from another primer extension experiment is shown by a separate gel (small box inside the gel). DNA sequence and transcripts ($P1_B$ to $P4_B$) are indicated on the left and right, respectively. (B) Total RNAs isolated from the wild type (lane 1), the wild type containing the *rdxBHIS* genes in pRK415 (lane 2), and the wild type containing the *rdxIS* genes in pRK415 (lane 3) were used for primer extension experiments with primer 101. The strains were grown aerobically. DNA sequence and transcript ($P1_I$) are indicated on the left and right, respectively. (C) The translational start site (designated +1) for *rdxB* is indicated with an arrow above the sequence which is shown in italics. A putative FnrL binding sequence is doubly underlined. (D) The translational start site (designated +1) for *rdxI* is indicated with an arrow above the sequence, which is shown in italics. The 5′ ends and directions are marked by arrows above the determined 5′ ends. The nucleotides mentioned above are in boldface. The binding sites of the primers used in the primer extension experiments are underlined with an arrow, and the numbers under the arrows indicate the primers used for the experiments.

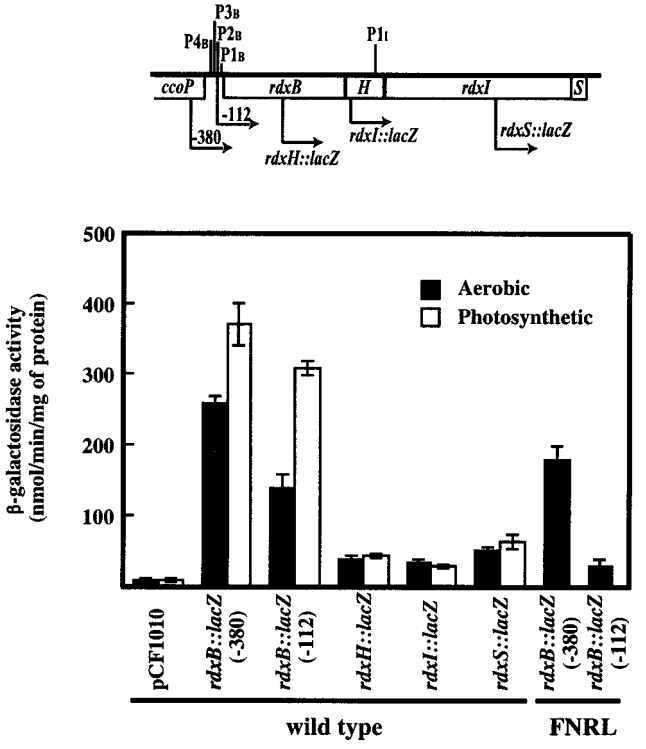

FIG. 5. β-Galactosidase activities of the various *rdxBHIS*::*lacZ* fusions in the wild-type and *fnrL* mutant strains. The positions of relevant RNA 5′ ends and 5′ endpoints of *lacZ* fusions are indicated. Strains were grown aerobically (sparged with 69% N_2–30% O_2–1% CO_2) and photosynthetically (sparged with 95% N_2–5% CO_2) to an OD_{600} of 0.4 ± 0.1. Activities are expressed as nanomoles of *o*-nitrophenyl-β-D-galactopyranoside hydrolyzed per minute per milligram of protein extract. Values with the ranges indicated are the average of two independent determinations. pCF1010 is the control plasmid vector containing the promoterless *lacZ* used to construct the *rdxBHIS*::*lacZ* fusions as described in Materials and Methods. Error bars indicate standard deviations.

termined a 5′ end at −79 bp upstream of the *rdxI* translational start (Fig. 4B). When extra copies of the *rdxBHIS* and *rdxIS* genes were used, the band for $P1_I$ increased approximately 2.5- to 3-fold (Fig. 4B, lanes 2 and 3) compared to wild type (lane 1), whereas there were no changes observed for the minor bands, which are not believed to be significant.

(iii) *lacZ* fusion analysis. In light of the report that each gene of the *ccoGHIS* cluster of *R. capsulatus* is expressed separately (9), we constructed *lacZ* fusion plasmids carrying DNA sequences upstream of each gene as determined from the preceding experiments. For the *rdxB*::*lacZ* fusion, we made two fusion plasmids, pJR316 and pJR319, containing sequences for all reported 5′ ends and for $P1_B$ alone, respectively. The *rdxB*::*lacZ*, *rdxH*::*lacZ*, *rdxI*::*lacZ*, and *rdxS*::*lacZ* fusions were introduced into *R. sphaeroides* 2.4.1, and β-galactosidase activities were determined (Fig. 5). The results demonstrated that each of the *rdxB*, *rdxH*, *rdxI*, and *rdxS* genes could be individually expressed, as reported for the *R. capsulatus ccoGHIS*, although only the *rdxB* fusion showed high expression for both aerobically and photosynthetically grown cells, which agrees with both the Northern and 5′-end analyses. Also, the −112 fusion showed lower β-galactosidase activities than the −380 fusion under these same conditions. The *lacZ* activities for the *rdxH*, *rdxI*, and *rdxS* fusions were all very low and showed little variation when assayed in cells grown aerobically or photosynthetically. In the *fnrL* mutant, β-galactosi-

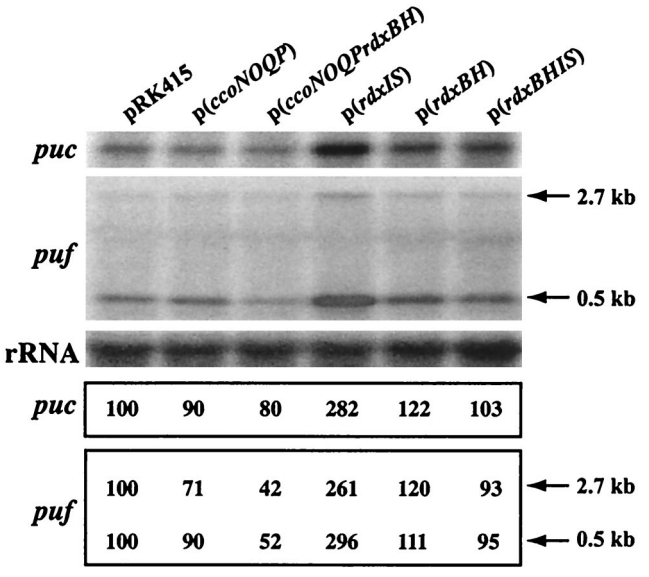

FIG. 6. Northern blot analysis of *R. sphaeroides* 2.4.1 grown under aerobic conditions. Total RNA was isolated from the wild type containing pRK415, the wild type containing *ccoNOQP* in pRK415 [p(*ccoNOQP*)], the wild type containing *ccoNOQP-rdxBH* in pRK415 [p(*ccoNOQP-rdxBH*)], the wild type containing *rdxIS* in pRK415 [p(*rdxIS*)], the wild type containing *rdxBH* in pRK415 [p(*rdxBH*)], and the wild type containing *rdxBHIS* in pRK415 [p(*rdxBHIS*)]. The strains were grown in Sistrom's minimal medium A containing tetracycline, by sparging with 69% N_2–30% O_2–1% CO_2, to an OD_{600} of 0.3 ± 0.05. Approximately 10 μg of total RNA was loaded onto each lane. Riboprobes specific for *puf*, *puc*, and the 23S rRNA gene were used for hybridization as described in Materials and Methods. The 2.7- and 0.5-kb transcripts for *puf* are present (6, 11). The levels of *puc* and *puf* were normalized to the level of rRNA. The mRNA level in the wild type containing pRK415 was considered 100%, and other values are given relative to that value.

dase activity for *rdxB*::*lacZ*(−112) was strongly suppressed, again suggesting FnrL regulation of the $P1_B$ transcriptional start. In the *fnrL* mutant, β-galactosidase activity for *rdxB*::*lacZ*(−380) was higher than that for *rdxB*::*lacZ*(−112). However, in the *fnrL* mutant grown aerobically, the −112 fusion showed the most significant decrease in β-galactosidase activity, suggesting the possible existence of a regulator(s) for aerobic activation of $P1_B$ in this region (between −380 and −112 bp) in addition to FnrL.

Cotranscription is important to photosynthesis gene expression. Our results strongly suggest that the *ccoNOQP-rdxBHIS* loci are transcribed predominantly as *ccoNOQP*, *ccoNOQP-rdxBH*, *rdxBH*, and *rdxIS*. To determine the potential role(s) of each transcript, plasmids which carried *ccoNOQP*, *ccoNOQP-rdxBH*, *rdxBHIS*, *rdxBH*, and *rdxIS* in pRK415 were constructed, and each plasmid was introduced into *R. sphaeroides* 2.4.1. *R. sphaeroides* 2.4.1 containing the *rdxIS* genes in pRK415 displayed a more intense red coloration under aerobic conditions than the other strains. Because we showed previously that colony coloration was related to the amount of spectral complexes formed under aerobic conditions (15–18, 20, 23), we determined the expression levels of the *puf* and the *puc* operons from these cells grown under aerobic conditions. As shown in Fig. 6, extra copies of *rdxIS* in *trans* (fourth lane) caused the highest expression levels for both *puf* and *puc* compared to the other strains. However, the effect of *rdxIS* overexpression was diminished by the presence of the *rdxBH* genes, which by themselves have very little effect (fifth and sixth lanes), suggesting that the stoichiometry of *rdxBH* and *rdxIS* expression is a critical factor in modulating photosynthesis gene expression. The levels of *puc* and *puf* expression were further decreased (Fig. 6) by overexpression of *ccoNOQP-rdxBH* compared to in the presence of *ccoNOQP* (17, 18).

DISCUSSION

The *ccoNOQP* operon, encoding the cbb_3 cytochrome *c* terminal oxidase, and the *rdxBHIS* gene cluster, whose gene products are involved in the structure and function of the cbb_3-type cytochrome *c* oxidase, are adjacent and lie in the same transcriptional orientation on chromosome I of *R. sphaeroides* 2.4.1 (16, 20, 22). Earlier complementation experiments using an *rdxB*::Tp mutation suggested the presence of a promoter internal to the gene cluster *rdxBHIS* (16). In this study, using Northern blot analysis (Fig. 1) and RT-PCR (Fig. 2), we have shown that the *ccoNOQP-rdxBHIS* cluster is transcribed as a *ccoNOQP-rdxBH*, *ccoNOQP*, *rdxBH*, and *rdxIS* series of transcripts. Using *lacZ* fusions, we have shown that each of the *rdxHIS* genes can be expressed separately at very low levels whose physiologic relevance is questionable. We cannot completely exclude the possibility of the presence of a low-abundance, unstable *rdxBHIS* transcript. However, the transcript would be rare, if it exists, because the expected 4.3-kb *rdxBHIS* transcript was not detected in either the *ccoN*::Km or the *ccoP*::Tp mutant strains. Further, the demonstration of the presence of a *ccoNOQP-rdxBH* transcript supports the conclusion that these are likely to represent the major source of expression of the *rdxBHIS* cluster. These results also reveal that expression of these gene clusters in *R. sphaeroides* is quite different from the expression patterns observed for *R. capsulatus* (9) and *S. meliloti* (7).

Since the cbb_3 cytochrome *c* oxidase is the main respiratory enzyme under microaerobic conditions and deficiency of the RdxHIS gene products causes a loss of the cbb_3 cytochrome *c* oxidase activity (20), coordination of the expression of *ccoNOQP-rdxBHIS* is likely to be precisely regulated in order to optimize energy production under these conditions. Previously, we reported that expression of *ccoNOQP* was dependent upon FnrL and was highest under semiaerobic conditions, moderate under photosynthetic conditions, and lowest under aerobic conditions (13). We have earlier shown that FnrL is required for expression of the photosynthesis genes, such as *puc*, *hemA*, *hemN*, *hemZ*, and *bchE*, in addition to expression of *ccoNOQP*, *rdxBHIS*, and *dorS*, which in turn affects the presence of dimethyl sulfoxide reductase (13, 19, 22). Thus, an *fnrL* mutant is unable to grow anaerobically, either photosynthetically or in the dark using dimethyl sulfoxide as an electron acceptor (22).

To understand how FnrL is involved in the regulation of *ccoNOQP* expression, we performed primer extension experiments with both the wild-type and the *fnrL* mutant strain (Fig. 3). Five *ccoNOQP* 5′ ends, designated $P1_N$, $P2_N$, $P3_N$, $P4_N$, and $P5_N$, were identified by primer extension analysis and are located at −53 bp, −82 bp, −109 bp, −110 bp, and −300 bp upstream of the *ccoN* translation start, respectively. Since

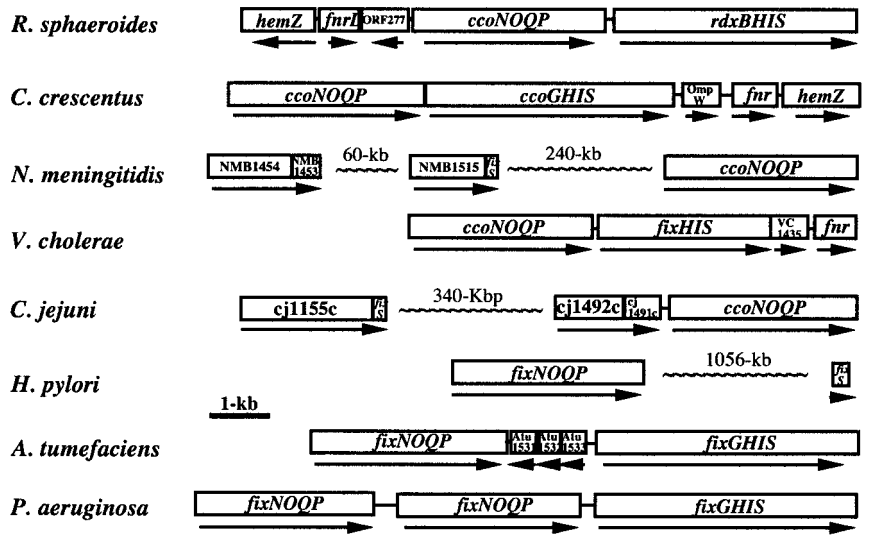

FIG. 7. Diagrams illustrating the genetic organization of the *cco*(*fix*)*NOQP-rdxBHIS* (*fix*/*ccoGHIS*) cluster and their flanking regions in different organisms. Homology searching was done with *rdxH* and *rdxS* because *rdxB* and *rdxI* have high homology to bacterial ferredoxin and CPx-type metal transporter which are normally found in many other bacteria. The DDBJ/EMBL/GenBank accession numbers of the sequences are as follows: *R. sphaeroides*, U58092 and AF202779; *Caulobacter crescentus*, AE005673; *Neisseria meningitidis*, AE002098 and AL162759; *Vibrio cholerae*, AE004222; *Campylobacter jejuni*, AL111168; *Helicobacter pylori*, AE001439 and AE000511; *Agrobacterium tumefaciens*, AE007869 and AE008688; and *Pseudomonas aeruginosa*, AE004091. *C. crescentus* OmpW is a putative outer membrane protein. The *fnrL* and *fnr* genes encode anaerobic transcriptional regulators. NMB1454 and NMB1453 are *rdxBH* homologues. VC1435 and Atu1531 are hypothetical proteins, and *hemZ* corresponds to the genes encoding isoenzymic forms of coproporphyrinogen III oxidase. NMB1515, which is composed of 436 amino acids, shows similarity to the central and carboxyl regions of the *R. sphaeroides* RdxI protein (737 amino acids) and is a putative transporter. cj1492c-cj1491c is a two-component regulatory system. cj1155c is an *rdxI* homologue. Atu1532 and Atu1533 are proteins related to glyoxylate and bleomycin resistance. The *rdxB* homologue of *V. cholerae* and the *rdxB* and *rdxI* homologues of *H. pylori* are not indicated. The *rdxH* homologue was not found for *H. pylori.*

β-galactosidase activity of a *ccoN*::*lacZ* fusion was significantly diminished in the *fnrL* mutant strain (13), in which the $P1_N$ transcript is absent, we suggest that $P1_N$ is both the major transcriptional start site for the *ccoNOQP* operon and positively regulated by FnrL. This pattern of *cco* transcription is entirely consistent with the previous determinations of β-galactosidase activity of *ccoN*::*lacZ* fusion-containing strains (13). Further, these data show that the *R. sphaeroides* FnrL is functional under aerobic conditions, although not as strongly as under microaerobic conditions. The aerobic activity of *R. sphaeroides* FnrL has been noted earlier and explained previously (22), when comparisons to a mutant form of the *E. coli* Fnr, which is oxygen stable, were made (10). *R. sphaeroides* FnrL possesses a histidine residue at position 29 and an alanine residue at position 154 that appear to influence oxygen stability of the *E. coli* Fnr.

Two FnrL binding motifs were centered at positions −41.5 and −73.5 relative to the $P1_N$ transcript site and at −11.5 and −43.5 from $P2_N$. Although FnrL functions as a major regulator of $P1_N$ expression, $P2_N$ expression was not affected in the *fnrL* mutant. Because the second FnrL binding motif (−43.5) from $P2_N$ is very close to the typical class II position (−41.5), additional experiments involving site-directed mutagenesis will be required to determine how the two FnrL motifs participate in the regulation of *ccoNOQP* expression. Although the other four start sites were similarly expressed in the *fnrL* and the wild type, transcription from the $P5_N$ start site appeared to involve another, unknown regulator(s). Inspection of the DNA sequence immediately preceding the $P5_N$ start site reveals sequence similarity to the *E. coli* σ^{54} promoter consensus sequence (1) (Fig. 3C). Experiments to confirm whether *R. sphaeroides* σ^{54} participates in *ccoNOQP* expression are in progress.

rdxB also has an FnrL binding motif at −42.5 bp from $P1_B$ (Fig. 4). Primer extension experiments and β-galactosidase activity of an *rdxB*::*lacZ* fusion (−112) demonstrate that transcription from $P1_B$ is positively regulated by FnrL (Fig. 4 and 5). The β-galactosidase activity of an *rdxB*::*lacZ* fusion (−380) in the *fnrL* mutant strain was approximately 70% of that in the wild type. Together, these results suggest that FnrL plays a role in *rdxB* expression under these conditions. Because expression of the two *rdxB*::*lacZ* fusions was high under photosynthetic conditions but differentially expressed in the absence of FnrL under aerobic conditions, we suggest that the presence of some unknown regulator(s) is also involved in the aerobic expression of *rdxB*.

The presence of multiple promoters for *ccoNOQP-rdxBHIS* expression suggests that expression of the *cco-rdx* cluster is tightly coordinated, depending upon the growth conditions, in order to permit the cells to adapt rapidly to the onset of environmental changes and to ensure proper cellular levels of the cbb_3 cytochrome *c* oxidase, which is essential for growth and regulation of photosynthesis gene expression under these different conditions.

Overexpression of *rdxIS* (Fig. 6) in *R. sphaeroides* 2.4.1 increased formation of the photosystem under aerobic conditions. Similarly, an *rdxI* in-frame deletion mutation showed spectral complexes under aerobic conditions, resulting from

the instability of the cbb_3 cytochrome oxidase (20). We suggested that RdxI is involved in the assembly and therefore the activity of the cbb_3 cytochrome oxidase through the maintenance of copper homeostasis (20). RdxS was also shown to have an effect on the steady-state presence of the cbb_3 cytochrome oxidase (20). Thus, either the absence or excess of the RdxIS gene products turns on photosynthesis gene expression under aerobic conditions, suggesting that these conditions can interfere with the structure-function of the cbb_3 oxidase, which in turn gives rise to photosynthesis gene expression such as when the *cco* operon is inactivated. In the closely related bacterium *R. capsulatus*, a CcoS (RdxS) mutant gives rise to a form of the cbb_3 cytochrome oxidase lacking heme *b*, heme b_3, and the copper cofactors of subunit I (9). Thus, we assume that the phenotype resulting from *rdxIS* overexpression is related to the cofactor state of the cbb_3 cytochrome oxidase.

Interestingly, *rdxBHIS* overexpression does not show the phenotype(s) which characterizes *rdxIS* overexpression (Fig. 6). This result suggests that *rdxBH* compensates for the effect of *rdxIS* overexpression, perhaps by establishing an appropriate stoichiometry for these gene products. In the *rdxB* in-frame deletion mutant, the cbb_3 cytochrome *c* oxidase was not affected in either activity or protein composition (17, 20). This mutant, however, does show photosynthesis gene expression under aerobic conditions. Thus, the physiological roles of RdxB and RdxH, -I, and -S must be distinct. One intermediate which transmits the inhibitory signal from the cbb_3 cytochrome oxidase to the PrrBA two-component system (2, 4, 5) in the presence of O_2, namely, PrrC has been identified (3). Are there others? RdxB has high homology to the bacterial ferredoxins, most likely containing a 2[4Fe-4S] cluster and two potential half centers (20). Because overexpression of *ccoNOQP-rdxBH* further represses photosynthesis gene expression under aerobic conditions, it is possible that electrons may be transferred via the cbb_3 cytochrome oxidase to RdxBH, which in turn may indirectly regulate PrrB activity.

Finally, database searches revealed both similar and dissimilar gene organizations for the *ccoNOQP-rdxBHIS* cluster in a variety of bacteria (Fig. 7). This diversity in the structure of the *ccoNOQP-rdxBHIS* loci in these various bacteria is interesting in its own right and likely reflects specific physiological requirements. But more importantly from the data presented here, it is apparent that these diverse gene organizations may reflect the need to provide gene products in alternative forms and abundances.

ACKNOWLEDGMENTS

This work was supported by a grant (GM15590) from the Public Health Service to S.K.

REFERENCES

1. **Barrios, H., B. Valderrama, and E. Morett.** 1999. Compilation and analysis of σ^{54}-dependent promoter sequences. Nucleic Acids Res. **27:**4305–4313.
2. **Eraso, J. M., and S. Kaplan.** 1996. Complex regulatory activities associated with the histidine kinase PrrB in expression of photosynthesis genes in *Rhodobacter sphaeroides* 2.4.1. J. Bacteriol. **178**:7037–7046.
3. **Eraso, J. M., and S. Kaplan.** 2000. From redox flow to gene regulation: role of the PrrC protein of *Rhodobacter sphaeroides* 2.4.1. Biochemistry **39**:2052–2062.
4. **Eraso, J. M., and S. Kaplan.** 1995. Oxygen-insensitive synthesis of the photosynthetic membranes of *Rhodobacter sphaeroides*: a mutant histidine kinase. J. Bacteriol. **177:**2695–2706.
5. **Eraso, J. M., and S. Kaplan.** 1994. *prrA*, a putative response regulator involved in oxygen regulation of photosynthesis gene expression in *Rhodobacter sphaeroides*. J. Bacteriol. **176:**32–43.
6. **Gong, L., J. K. Lee, and S. Kaplan.** 1994. The Q gene of *Rhodobacter sphaeroides*: its role in *puf* operon expression and spectral complex assembly. J. Bacteriol. **176:**2946–2961.
7. **Kahn, D., M. David, O. Domergue, M. L. Daveran, J. Ghai, P. R. Hirsch, and J. Batut.** 1989. *Rhizobium meliloti fixGHI* sequence predicts involvement of a specific cation pump in symbiotic nitrogen fixation. J. Bacteriol. **171:**929–939.
8. **Keen, N. T., S. Tamaki, D. Kobayashi, and D. Trollinger.** 1988. Improved broad-host-range plasmids for DNA cloning in gram-negative bacteria. Gene **70:**191–197.
9. **Koch, H. G., C. Winterstein, A. S. Saribas, J. O. Alben, and F. Daldal.** 2000. Roles of the *ccoGHIS* gene products in the biogenesis of the cbb_3-type cytochrome *c* oxidase. J. Mol. Biol. **297:**49–65.
10. **Lazazzera, B. A., D. M. Bates, and P. J. Kiley.** 1993. The activity of the *Escherichia coli* transcription factor FNR is regulated by a change in oligomeric state. Genes Dev. **7:**1993–2005.
11. **Lee, J. K., B. S. DeHoff, T. J. Donohue, R. I. Gumport, and S. Kaplan.** 1989. Transcriptional analysis of *puf* operon expression in *Rhodobacter sphaeroides* 2.4.1 and an intercistronic transcription terminator mutant. J. Biol. Chem. **264:**19354–19365.
12. **Lee, J. K., and S. Kaplan.** 1995. Transcriptional regulation of *puc* operon expression in *Rhodobacter sphaeroides*. Analysis of the *cis*-acting downstream regulatory sequence. J. Biol. Chem. **270:**20453–20458.
13. **Mouncey, N. J., and S. Kaplan.** 1998. Oxygen regulation of the *ccoN* gene encoding a component of the cbb_3 oxidase in *Rhodobacter sphaeroides* $2.4.1^T$: involvement of the FnrL protein. J. Bacteriol. **180:**2228–2231.
14. **Neidle, E. L., and S. Kaplan.** 1992. Rhodobacter sphaeroides *rdxA*, a homolog of *Rhizobium meliloti fixG*, encodes a membrane protein which may bind cytoplasmic [4Fe-4S] clusters. J. Bacteriol. **174:**6444–6454.
15. **O'Gara, J. P., J. M. Eraso, and S. Kaplan.** 1998. A redox-responsive pathway for aerobic regulation of photosynthesis gene expression in *Rhodobacter sphaeroides* 2.4.1. J. Bacteriol. **180**:4044–4050.
16. **O'Gara, J. P., and S. Kaplan.** 1997. Evidence for the role of redox carriers in photosynthesis gene expression and carotenoid biosynthesis in *Rhodobacter sphaeroides* 2.4.1. J. Bacteriol. **179**:1951–1961.
17. **Oh, J. I., and S. Kaplan.** 1999. The cbb_3 terminal oxidase of *Rhodobacter sphaeroides* 2.4.1: structural and functional implications for the regulation of spectral complex formation. Biochemistry **38:**2688–2696.
18. **Oh, J. I., and S. Kaplan.** 2000. Redox signaling: globalization of gene expression. EMBO J. **19:**4237–4247.
19. **Oh, J. I., and S. Kaplan.** 2001. Generalized approach to the regulation and integration of gene expression. Mol. Microbiol. **39:**1116–1123.
20. **Roh, J. H., and S. Kaplan.** 2000. Genetic and phenotypic analyses of the *rdx* locus of *Rhodobacter sphaeroides* 2.4.1. J. Bacteriol. **182**:3475–3481.
21. **Simon, R., U. Priefer, and A. Puhler.** 1983. A broad host range mobilization system for in vivo genetic engineering: transposon mutagenesis in Gram negative bacteria. Bio/Technology **1:**37–45.
22. **Zeilstra-Ryalls, J. H., and S. Kaplan.** 1995. Aerobic and anaerobic regulation in *Rhodobacter sphaeroides* 2.4.1: the role of the *fnrL* gene. J. Bacteriol. **177:**6422–6431.
23. **Zeilstra-Ryalls, J. H., and S. Kaplan.** 1996. Control of *hemA* expression in *Rhodobacter sphaeroides* 2.4.1: regulation through alterations in the cellular redox state. J. Bacteriol. **178:**985–993.
24. **Zeilstra-Ryalls, J. H., and S. Kaplan.** 1998. Role of the *fnrL* gene in photosystem gene expression and photosynthetic growth of *Rhodobacter sphaeroides* 2.4.1. J. Bacteriol. **180**:1496–1503.